Zonda downslope winds in the central Andes of South America in a 20-yr climate simulation with the Eta model

Pablo L. Antico[1 2 3] * , Sin Chan Chou[4] and Caroline Mourão[5]

[1] Consejo Nacional de Investigaciones Científicas y Técnicas, Argentina.

[2] Departamento de Ciencias de la Atmósfera y los Océanos, Facultad de Ciencias Exactas y Naturales, Universidad de Buenos Aires, Intendente Güiraldes 2160, Ciudad Universitaria, C1428EGA, Argentina.

[3] Facultad de Ciencias Astronómicas y Geofísicas, Universidad Nacional de La Plata, Paseo del Bosque s/n, B1900FWA, Argentina.

[4] Instituto Nacional de Pesquisas Espaciais (INPE), Rod.Pres. Dutra, km 39, CEP 12630-000, Cachoeira Paulista, SP, Brasil.

[5] Centro Nacional de Monitoramento e Alertas de Desastres Naturais (CEMADEN), Rodovia Dutra, km 39, CEP 12630-000, Cachoeira Paulista, SP, Brasil.

* Corresponding author: E-mail: antico@at.fcen.uba.ar; Tel: (++54 +11) 4576-3356 ext. 22; Fax: (++54 +11) 4576-3356 ext. 12

ABSTRACT

The Zonda wind is a local version of the alpine foehn in the central Andes mountains in South America. It blows on the eastern slopes and produces an extremely warm and dry condition in Argentina. In this study, the occurrence of Zonda wind events during a 20-yr simulation from the regional Eta model is analyzed and results are compared to previous studies of Zonda wind events based on weather observations. We define a set of parameters to account for the zonal pressure gradient across the mountain, vertical movement and air humidity typical of Zonda wind events. These parameters are applied to characterize Zonda wind events in model run and to classify them as surface-level or high-level episodes.

The resulting annual distribution of Zonda occurrences based on composite analyses shows a preference for winter and spring with rare occurrences during summer. For the surface–level Zonda wind events, the highest frequency occurs during spring. Whereas surface–level Zonda wind episodes more commonly initiate in the afternoon, high–level Zonda wind events show no preference for a given initiation time. Our results are mostly in agreement with previous observational results.

Acknowledgments. This study was part of a research project performed at the Centro de Previsão do Tempo e Estudos Climáticos (CPTEC-INPE) of Brazil during the first author's visit. We are very grateful to Prof. Fedor Mesinger for valuable comments and suggestions which contributed to this work. This research was partially supported by grant PIP 2013-2015 GI11220120100586 from the Consejo Nacional de Investigaciones Científicas y Técnicas and by CNPq grants p308035/2013-5, 457874/2014-7 and 400792/2012-5.

1. Introduction

Downslope winds often blow east of the Andes Mountains, causing extremely warm and dry conditions, and at times strong gusts, property damage, adverse health effects, and other problems. This wind, which is a variant of the alpine foehn, is locally called 'Zonda wind' in reference to the name of the river valley where it normally occurs. It is a semi-permanent meteorological feature generally found aloft in the high mountains. The latter is called high–level Zonda wind (HGZ), distinguished from surface–level Zonda wind (SFZ) (Norte, 1988). Although Zonda wind may blow almost everywhere at extratropical latitudes downstream of the Andes, observations demonstrate that it is more common between 32º and 33ºS, near the cities of Mendoza and San Juan in Argentina (Norte 1988). The Andes mountain range extends from tropical to extratropical latitudes along the western edge of South America. North of approximately 35ºS, mountains are high enough (above 4,000 m) to block cold and wet air from the Pacific Ocean to the west of the Andes. Occasionally, air may rise, cross the mountains and descend onto the eastern slopes of the Andes. Thus, a Zonda wind episode develops, causing air warming and drying due to adiabatic compression (Seluchi et al. 2003). This process is accompanied by a mid-level tropospheric disturbance that crosses over the Andes and a polar jet stream associated to a cold front moving from the southwest. Ahead of the cold front, a surface low deepens as the upper-level trough moves eastward causing an intense zonal pressure gradient that accelerates downslope wind. Typical meteorological situations for different Zonda episodes have been extensively discussed in Seluchi et al. (2003) and Norte et al. (2008).

There are few studies about the Zonda wind, probably due to the scarcity of observational data in the mountains, particularly in the steep terrain of the Andes. A detailed description of the ‘state of the art’ research on Zonda wind is found in Norte (2015). The most exhaustive study about Zonda wind is that conducted by Norte (1988). He analyzed the occurrence of Zonda wind events during a 10-yr period based on weather observations. His Zonda wind definition included temperature, relative humidity, atmospheric pressure, wind, cloudiness and weather reports (e.g., sandstorm). He defined four categories of Zonda wind events as a function of maximum gusts, which ranged from moderate to extremely severe. Later, Seluchi et al. (2003) discussed the physical mechanisms for Zonda wind occurrence, and related the wind to stability parameters, vertical movement and zonal pressure gradients on both sides of the mountains. They classified Zonda wind in three categories: moderate and severe SFZ and HGZ. Norte (1988) found that 6 % of the HGZ episodes later became SFZ episodes and that most of them occurred during winter and spring. A few attempts were made to simulate the Zonda wind using numerical models. Seluchi et al. (2003) successfully simulated three different Zonda wind episodes with the Eta model. Later, Norte et al. (2008) used the RAMS model with quasi-horizontal coordinate surfaces to simulate a severe Zonda wind episode. Mesinger et al. (2012) described an upgraded version of the Eta model that includes the step-wise vertical advection scheme designed to increase the wind speed during downslope wind events. The latter refers to the problem that arises from the Mountain of Agnesi experiments performed by Gallus and Klemp (2000) when using the eta coordinate. In Mesinger et al. (2012) this problem was extrapolated to real situations of foehn-like winds and the Eta model was used to forecast the same Zonda episode studied by Norte et al. (2008). Despite the encouraging results obtained by Norte et al. (2008), results of Mesinger et al. (2012) are in better agreement with observations. They used a higher resolution horizontal (approx. 8 km) grid and assumed non-hydrostatic equilibrium. However, the authors state that hydrostatic approximation in the Eta model does not have a significant impact on the results. Hence, Mesinger et al. (2012) explained the successfully forecasted Zonda windstorm in terms of model refinements given by the sloping eta coordinate and the piecewise linear advection scheme, which is finite volume-like scheme for vertical advection of temperature.

Prior to using the Eta model for climate simulations of the Zonda winds, the objective of this work is to evaluate the simulation of Zonda wind events on the lee side of the Andes in a 20-yr simulation of the regional Eta model, by comparing the results to previous observational studies of Zonda wind events (Norte, 1988, 2015; Seluchi et al., 2003).

2. Methodology

We define and estimate a set of required parameters to determine Zonda wind events in the model simulation: the zonal pressure gradient across the mountain, the downward vertical movement, and the magnitude and vertical extent of the drying effect. Then we distinguish SFZ from HGZ events and analyze a selected case study. A composite analysis of all selected Zonda cases is performed. Results are presented in the form of vertical cross-sections through the Andes Mountains and frequency distributions at annual and hourly time frames.

2.1. Model setup

A climate simulation over South America was obtained from a 20-yr long integration of the upgraded version of the seasonal Eta model at INPE (Mesinger et al., 2012). Climatology was constructed from 6 hourly outputs during the period 1989-2008 over a domain encompassing South America and adjacent oceans with a horizontal resolution of approximately 50 km and 38 vertical levels. The first year of model integration corresponded to model spinup and was discarded. Hydrostatic equilibrium was assumed. Lateral boundary conditions were updated every 6 hours and were provided by ERA-Interim global analyses at 150-km horizontal resolution. Lower boundary conditions were provided by a four-layer soil model (NOAH) (Chen et al., 1997; Ek et al., 2003), using climatological soil moisture. Sea surface temperature was updated on a daily basis. For cumulus parameterization, the model adopted the Betts–Miller scheme modified by Janjic (1994), and for cloud microphysics, the Zhao scheme (Zhao et al. 1997).

2.2. Zonda wind definition

The methodology to identify Zonda wind events in the 20-yr simulation relies on pressure gradient, vertical movement, and humidity conditions. In addition, a fourth parameter is applied to distinguish the HGZ from the SFZ.

As noted by Seluchi et al. (2003), a necessary condition for downslope wind on the eastern slopes of the Andes is the existence of a zonal pressure gradient across the mountain range. To identify this gradient in the 20-yr simulation, a zonal pressure gradient index (ZPI) is defined as a difference of mean sea level pressure (MSLP) between two points, one located to the west (33°S 71°W) and the other to the east (33°S

68°W) of the Andes. The latter is near the city of Mendoza (704 m a.s.l., 32°50'S 68°47'W) where Zonda events frequently occur. The first condition to identify Zonda requires ZPI > 0, i.e. MSLP to the west must be greater than MSLP to the east of the Andes. This condition fulfills the requirement of an eastward directed pressure gradient across the mountain range.

One of the advantages of using numerical model output is the availability of vertical movement information at different pressure levels and at high frequency. Following Norte (1988), we chose the 700-hPa level as the level where maximum vertical movement occurs when Zonda wind blows. In addition, we define the ω_{700} index as the 700-hPa vertical movement taken at 33ºS 68ºW. The second condition to identify Zonda requires that ω_{700} be positive, i.e. downward vertical movement on the lee side of the Andes.

The adiabatic compression due to air descent causes warming and drying in the lower troposphere, which is more pronounced at the 850-hPa level (Norte, 1988). This condition suggests the use of the RH_{850} index, representing relative humidity at the 850 hPa level at grid point 33ºS 68ºW. Hence, the third condition for Zonda event occurrence requires that RH_{850} falls to 40%, in order to detect the drying process due to air descent downslope of the mountains. In addition, the ΔRH parameter is defined as the difference between the relative humidity at 850 hPa and at the surface (2 metres above ground) at 33ºS 58ºW. In the case that the descending dry air reaches the surface, RH does not significantly differ between the 850-hPa level and the surface. Finally, a fourth condition is applied to define the occurrence of a SFZ episode, which requires a ΔRH less than 15%, otherwise a Zonda episode is classified as HGZ. These thresholds were chosen to minimize subsidence effects not related to Zonda wind, as in the case of migratory anticyclones in westerly waves.

To summarize the aforementioned conditions for Zonda wind detection in the 20-yr simulation, a Zonda episode is defined when ZPI becomes positive, ω_{700} attains at least 1.0 hPa s^{-1}, and RH_{850} is smaller than 40%. Additionally, a Zonda episode is classified as SFZ when ΔRH index is below 15%.

3. Results

Prior to showing the general characteristics of the simulation of Zonda wind events, a particular case study is described in more detail as a verification of the detection scheme.

3.1. A case study: the SFZ event of 18 September 1995 in the 20-yr simulation

The synoptic pattern in the 1000-hPa isobaric chart at 00UTC (Figure 1a) exhibits an intense eastward zonal pressure gradient over the Andes north of 36ºS, which results in a ZPI value of 20.7 hPa. This gradient results from the action of an anticyclone on the Pacific Ocean at 35ºS and a low pressure center on the Atlantic Ocean at 44ºS near the coast. Between the zone of intense pressure gradient over the Andes and the Atlantic low, a baroclinic zone with cold advection denotes a cold front moving northeastward. A secondary low is located ahead of the cold front, to the northeast, at the latitude of the strong pressure gradient over the Andes. This pattern resembles the typical Zonda wind pattern described in previous studies (e.g., Seluchi et al. 2003) detected through surface charts.

At the 500-hPa level (Figure 1b), maximum wind blows across the Andes between 30ºS and 36ºS as a trough axis remains behind the low-level Atlantic low. Interaction between air flow and the mountains is verified by the vertical movement at 700-hPa (Fig. 1c) with a strong upslope flow just to the southwest of an area with intense downslope flow on the lee side. The southwest-northeast orientation of this dipole of negative-positive vertical movement responds to the mean direction of the flow just above the mountain (Fig. 1b) and to the polar jet position as shown in Figure 1d.

Figure 2a shows vertical movement across the Andes Mountains at 33ºS. The zonal wind component blows from the west over the entire domain (shown in Fig. 2b). The downward motion on the leeward side of the Andes is stronger than the upward motion on the windward side and can reach lower levels near the surface. This feature clearly represents a downslope wind, as it is supported by a ω_{700} value over 2.0 hPa s^{-1}. Figure 2b shows the vertical cross section of the zonal wind. Maximum wind is found at 250-hPa over the mountains and indicates the location of the polar jet previously described in Figure 1d.

The pseudoadiabatic equivalent potential temperature, θ_{ae} is conserved during a pseudoadiabatic process such as the one that takes place when an air mass rises upslope the mountains and produces precipitation. When this air mass crosses and descends on the leeward side of the mountain, as in the case of a Zonda wind event, θ_{ae} should be the same, as we assume that most of the moisture precipitated as rain or snow during the process. In this study, θ_{ae} is computed with the Eq. (6) of Bryan (2008).

During the Zonda wind event, θ_{ae} is approximately conserved during the ascent and descent over the Andes mountains (Fig. 3a) which indicates that the cold air of the lower troposphere over the Pacific Ocean crosses over the mountain top and descends (downslope) on the leeward side. This effect is shown by the pseudoadiabatic equivalent isentropes lower than 310 K from the mountain top over the lee side to the east, where θ_{ae} values are similar to those found to the west at lower levels over the Pacific Ocean. The potential temperature θ (Fig. 3b) across the Andes Mountains also confirms the Zonda occurrence. Cold and moist surface maritime air over the Pacific Ocean is forced to follow the western slopes in an ascending motion, resulting in a strong vertical gradient of θ. When this air descends downslope on the eastern side, the corresponding isentropes are vertically aligned, denoting a typical dry adiabatic of neutral vertical gradient associated with a SFZ episode (Seluchi et al. 2003). The vertical profile of relative humidity (RH) across the Andes is shown in Figure 4. RH values above 70% suggest cloudy air, as normally occurs over the Pacific Ocean and along the western slope of the Andes, where the air rises. Above the mountain top, the 70% contour of relative humidity describes a typical 'Zonda wall' described in figure 4 of Norte (2015) during moderate or severe surface Zonda wind episodes. The RH_{850} is 10% and ΔRH is 5%, which indicates a severe Zonda event that reaches the surface.

Figure 5a shows the 6-hour accumulated precipitation values during the Zonda event. As expected, precipitation occurs windward of the mountain slopes and also over the high mountains. Due to below-zero temperatures at high mountains, a fraction of this precipitation is snow (Figure 5b). As noted by Norte (1988), during a typical moderate to severe Zonda event, precipitation occurs on the windward slopes and heavy snow occurs over high mountains, which causes communication disruptions between Santiago and Mendoza cities , on both sides of the Andes.

3.2. Zonda wind composites

The composite of the Zonda events in the 20-yr simulation show similarities with the case study. The strongest vertical movements (Figure 6) occur just above the mountain top at 550 hPa on both sides, with an absolute maximum greater than 2 hPa s^{-1}. The composite of θ_{ae} across the Andes (Fig. 7a) clearly shows the 310-K isentrope above the mountain top descending to the east of the mountain, which denotes the effect of Zonda wind. The latter is also appreciated in the vertical alignment of the isentropes on the leeward side (Fig. 7b), as in the case of the 304 K isentrope, indicating neutral stability generated by adiabatic compression of descending air.

The occurrence of simulated Zonda episodes has a well defined annual cycle, as shown in Figure 8. Zonda events mostly occur during May–October, with rare occurrences during November–April. Noticeably, the maximum frequency of SFZ events is in September, while the maximum frequency of HGZ events is in July.

Because model outputs are available at 00, 12, 18, and 21 UTC, it is assumed that a Zonda episode initiates within the 6-hour time interval before the model output time. For example, if a Zonda event is detected at 18 UTC, the event probably initiated during the period between 12 UTC and 18 UTC, however, in this case the Zonda event initiation time is defined as 18 UTC. The local times are 20, 02, 08, and 14 hours, corresponding to 00, 06, 12, and 18 UTC, respectively.

Daily distribution of initiation time of Zonda episodes are presented in Figure 9. When considering the total number of Zonda episodes, there is a preference for 00 UTC as the initiation time. This maximum is mostly explained by the contribution of SFZ episodes, which generally initiate during the afternoon (i.e. between 14 and 20 local time).

Norte (1988) demonstrates that SFZ events commonly initiate during the afternoon, which agrees with our results. Seluchi et al. (2003) attribute this characteristic to thermal turbulence during daytime on the leeward side of the mountain. This condition would break or weaken subsidence inversion and favor the Zonda wind reaching the ground. A climatology of Zonda wind occurrence based on 30-yr hourly surface observations at Mendoza city is presented in Norte (2015). His results are also in agreement with our results presented in Figures 8 and 9.

4. Conclusions

Results presented in this study are a first climatological study of Zonda wind events made from a 20-yr long-term simulation over South America using the regional Eta model. Comparison with observational results from previous studies demonstrates that the Eta model properly simulates the foehn-like effect on the eastern slopes of the highest Andes mountains.

A set of parameters with the corresponding thresholds are defined at a point located near the city of Mendoza in Argentina. These are applied to classify Zonda wind events as SFZ or HGZ episodes. A SFZ case study simulated by the model was used to validate the adopted criteria for Zonda event definition used in this work.

The annual distribution of Zonda wind occurrences obtained from composite analyses shows a preference for winter and spring with almost no occurrences during summer. The occurrence of SFZ events has a maximum frequency during spring. When analyzing the initiation time of Zonda wind events, there is almost no preference for a given initiation time in the case of HGZ events, i.e. they may initiate at any time during day. However, SFZ episodes have a preferred initiation time in the afternoon, and rarely initiate at night or in the morning. Surprisingly, both the annual distribution and the preferred initiation time for Zonda wind events are mostly in agreement with previous studies based on observational data (Norte, 2015). However, in the Zonda climatology of Norte (1988), only 6% of Zonda wind events became surface episodes, in contrast with 34% in our results. This difference is probably due to different criteria adopted in each study to define Zonda wind events. Whereas during real SFZ events, strong wind gusts are usually observed, the Eta model provides average wind velocities, rather than wind gusts values. For these reasons, we choose the vertical extent of lower tropospheric dry air instead of wind velocity to distinguish between SFZ and HGZ events. This condition imposes a limitation on our results in terms of windstorm severity, but the results show that Zonda-related dryness is captured by the model.

Further research is needed to analyze the regional extent of the Zonda wind effect along the entire range of the eastern slopes of the Andes Mountains. These results can be extended to other regions of South America where downslope winds may also occur. The climatology of Zonda wind events can contribute to assess its impacts on human activities, not only in terms of destructive windstorms but also to control air dryness in vineyards and fruit production, two of the most important economic activities in the region.

List of Acronyms and Parameters

HGZ : High-level Zonda wind

SFZ : Surface-level Zonda wind

ZPI : Zonal pressure gradient index

ω_{700} : 700-hPa vertical movement index

RH_{850} : 850-hPa relative humidity index

ΔRH : Surface relative humidity minus RH_{850}

θ_{ae} : Pseudoadiabatic potential temperature

θ : Potential temperature

RH : relative humidity

References

Bryan GH (2008) On the computation of pseudoadiabatic entropy and equivalent potential temperature. Mon Wea Rev 136: 5239-5245.

Chen F, Janjić ZI, Mitchell K (1997) Impact of atmospheric surface-layer parameterization in the new land-surface shceme of the NCEP mesoscale Eta Model. Bound-Layer Meteor 85: 391-421.

Ek MB, Mitchell KE, Lin Y, Rogers E, Grummen P, Koren V, Gayno G, Tarpley JD (2003) Implementation of NOAH land surface advances in the National centers for environmental prediction operational mesoscale Eta model. J Geophys Res 108: 8851. doi:10.1029/2002JD003246.

Gallus WA, Klemp JB (2000) Behavior of flow over step topography. Mon Wea Rev 128: 1153-1164.

Janjic ZI (1994) The setp-mountain eta coordinate model: further developments of the convection, Viscous sub layer and turbulence closure schemes. Mon Wea Rev 122: 927-945.

Mesinger F, Chou SC, Gomes JL, Jovic D, Bastos P, Bustamente JF, Lazic L, Lyra AA, Morelli S, Ristic I, Veljovic K (2012) An upgraded version fo the Eta model. Meteorol Atmos Phys 116:63–79. doi 10.1007/s00703-012-0182-z.

Norte FA (1988) Características del Viento Zonda en la Región de Cuyo [Zonda wind features at Cuyo region, *T*]. PhD dissertation, University of Buenos Aires.

Norte FA (2015) Understanding and Forecasting Zonda Wind (Andean Foehn) in Argentina: A Review. Atmospheric and Climate Sciences 5: 163-193. http://dx.doi.org/10.4236/acs.2015.53012

Norte FA, Ulke AG, Simonelli SC, Viale M (2008) The severe zonda wind event of 11 July 2006 east of the Andes Cordillera (Argentine): a case study using the BRAMS model. Meteorol Atmos Phys 102: 1–14. doi 10.1007/s00703-008-0011-6.

Seluchi ME, Norte FA, Satyamurty P, Chou SC (2003) Analysis of three situations of the Foehn effect over the Andes (Zonda Wind) using the Eta–CPTEC regional model. Wea Forecasting 18: 481-501.

Zhao Q, Black TL, Baldwin ME (1997) Implementation of the cloud prediction scheme in the Eta model at NCEP. Weather Forecast 12: 697-712.

FIGURE CAPTIONS

Fig. 1 Zonda wind event during the 20-yr simulation from the Eta model corresponding to September 18, 1995 at 00UTC; (a) 1000-hPa geopotential height (gpm, solid line) and wind vector (reference vector is 30 m s^{-1}), and 500–1000-hPa layer thickness (gpm, dashed line); (b) 500-hPa geopotential height (gpm, solid line) and wind velocity (m s^{-1}, grey shadows); (c) 700-hPa vertical movement (hPa s^{-1}, dashed line for negative values less than –1 hPa s^{-1} and solid line for positive values greater than 1 hPa s^{-1}, contour interval is 0.5 hPa s^{-1}); and (d) 250-hPa streamlines and wind velocity (m s^{-1}, grey shades).

Fig. 2 Vertical cross section at 33ºS for a Zonda wind event during the 20-yr simulation from the Eta model corresponding to September 18, 1995 at 00UTC; (a) vertical movement in hPa s^{-1} (solid line for positive values and dashed line for negative values, thick solid line for zero contour); (b) zonal wind in m s^{-1} (solid line). Surface topography is identified as black vertical bars.

Fig. 3 As in Fig. 2 but for; (a) pseudoadiabatic equivalent potential temperature in K (solid line, thick line each 10 K); and (b) potential temperature in K (solid line).

Fig. 4 As in Fig. 2a but for relative humidity (%, solid line). Light-blue shading indicates relative humidity values greater than 70% and dark-yellow shading less than 10%.

Fig. 5 Six-hour accumulated precipitation (mm/6h) during a Zonda wind event in the 20-yr simulation from the Eta model prior to September 18, 1995 at 00UTC (panel a). Snowfall in mm/6h (panel b).

Fig. 6 Vertical cross section at 33ºS of vertical movement composite for the surface Zonda wind episodes (*n* = 64) corresponding to ω_{700} = 1.0 hPa s^{-1}, RH_{850} = 40 % and ΔRH = 15% of the 20-yr simulation from the Eta model. Solid (dashed) line for positive (negative) values. Contour interval is 0.5 hPa s^{-1}, thick solid line for zero contour and surface topography is shaded in black.

Fig. 7 As in Fig. 6 but for; (a) pseudoadiabatic equivalent potential temperature in K (solid line, thick line every 10 K); and (b) potential temperature in K (solid line).

Fig. 8 Annual frequency of Zonda wind occurrences in the 20-yr simulation from the Eta model considering ω_{700} = 1.0 hPa s^{-1} and RH_{850} = 40 % (black). For SFZ events, the adopted criteria is ΔRH = 15% (white).

Fig. 9 Diurnal frequency of the initiation time of Zonda wind events in the 20-yr simulation from the Eta model considering ω_{700} = 1.0 hPa s^{-1} and RH_{850} = 40 % (black). For SFZ events, the adopted criteria is ΔRH = 15% (white). Vertical axis values are absolute frequencies; horizontal axis values are model output times expressed in UTC (upper line) and local time (bottom line).

Figure

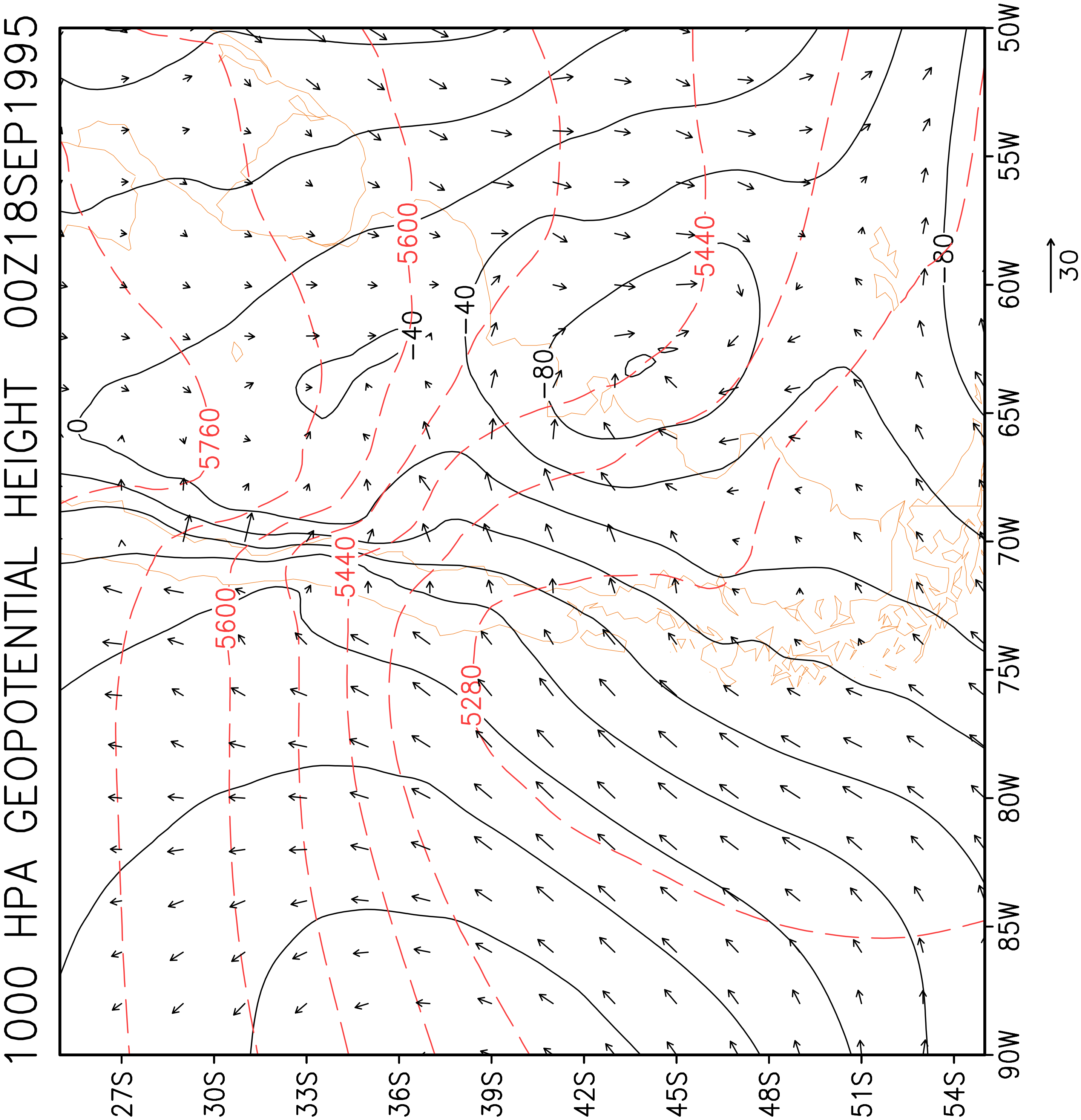
1000 HPA GEOPOTENTIAL HEIGHT 00Z18SEP1995
27S
30S
33S
36S
39S
42S
45S
48S
51S
54S
90W
85W
80W
75W
70W
65W
60W
55W
50W
30
0
-40
-80
5760
5600
5440
5280

Figure

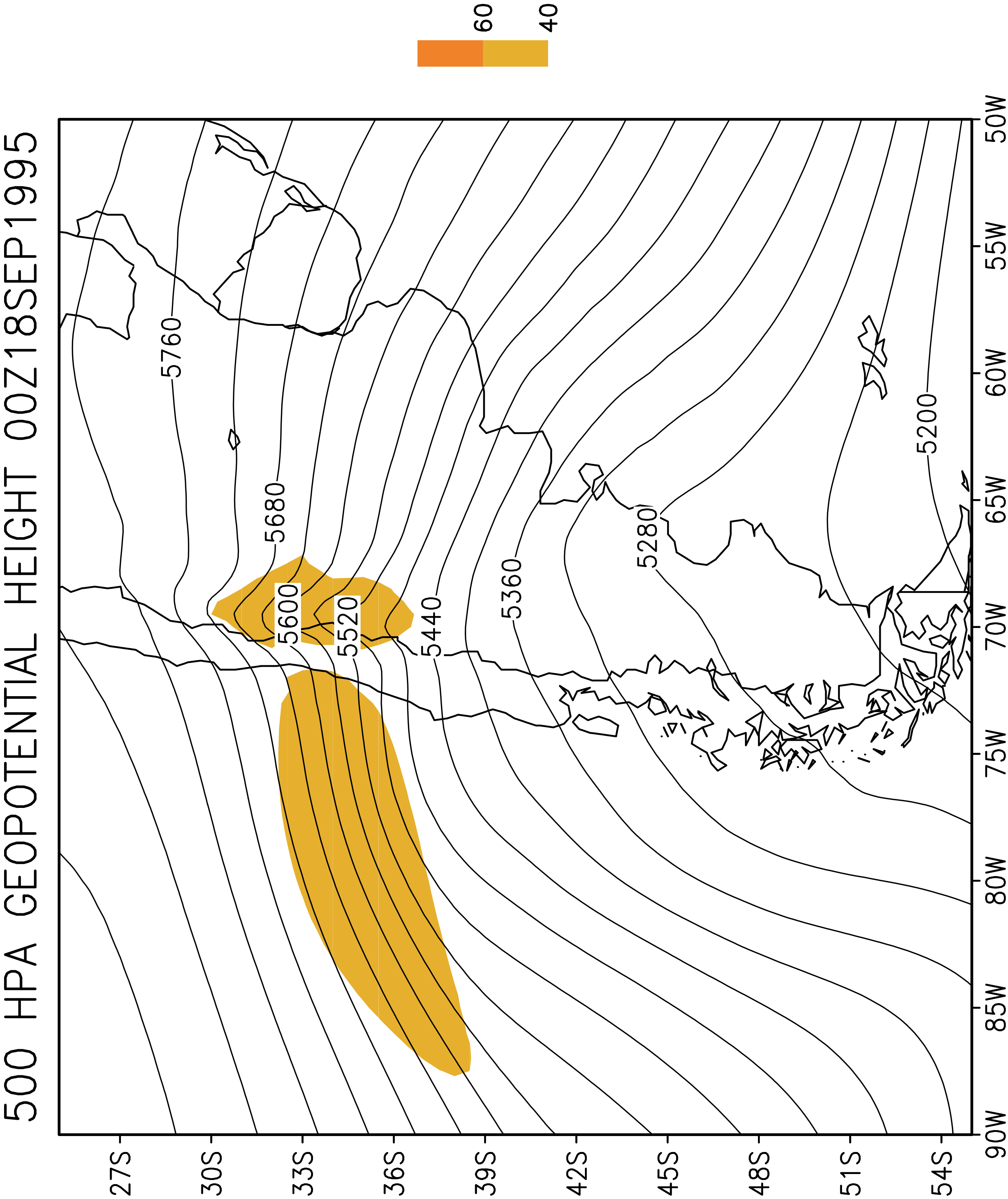
500 HPA GEOPOTENTIAL HEIGHT 00Z18SEP1995
60
40
5760
5680
5600
5520
5440
5360
5280
5200
27S
30S
33S
36S
39S
42S
45S
48S
51S
54S
90W
85W
80W
75W
70W
65W
60W
55W
50W

Figure

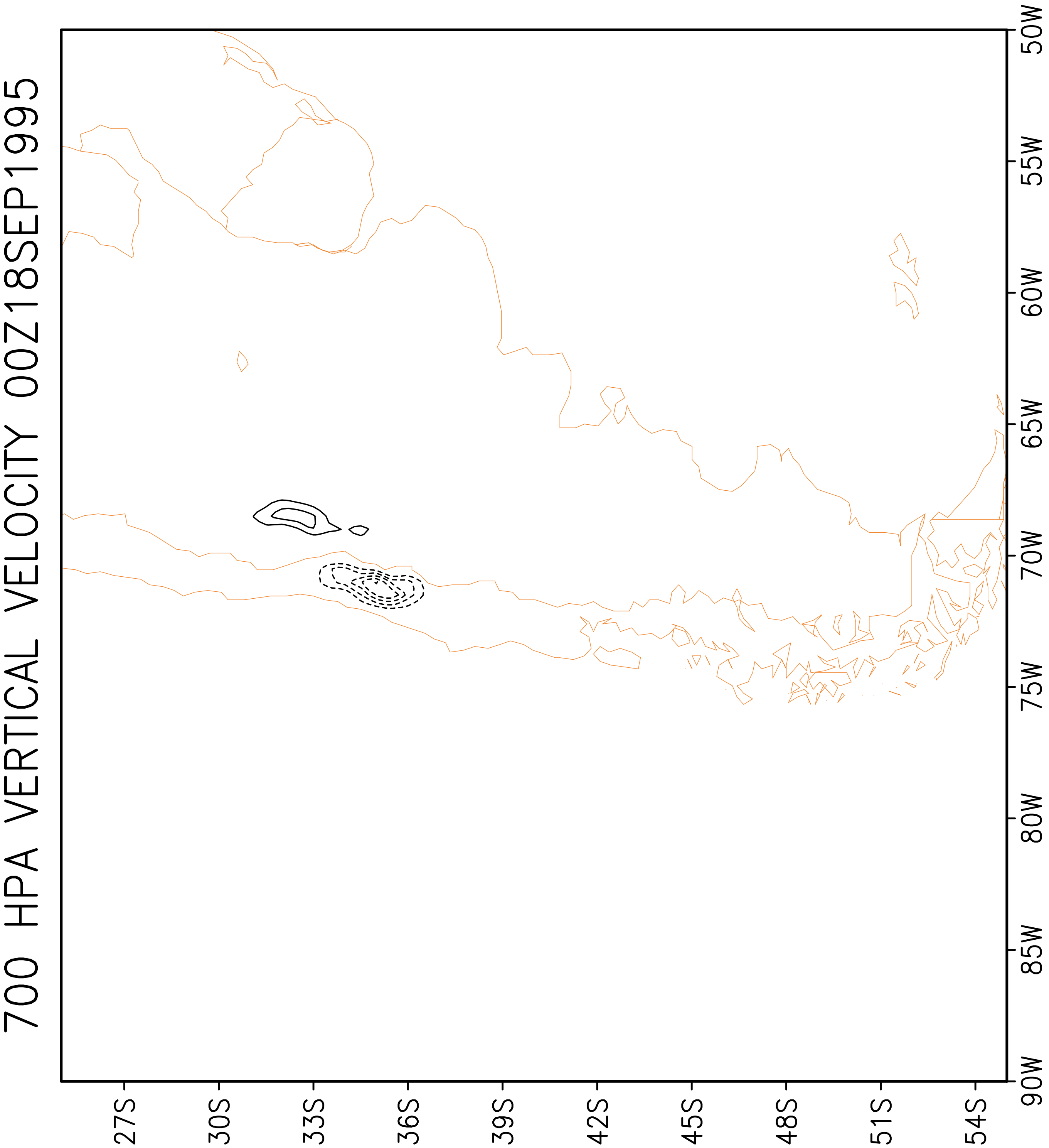
700 HPA VERTICAL VELOCITY 00Z18SEP1995
50W
55W
60W
65W
70W
75W
80W
85W
90W
27S
30S
33S
36S
39S
42S
45S
48S
51S
54S

Figure

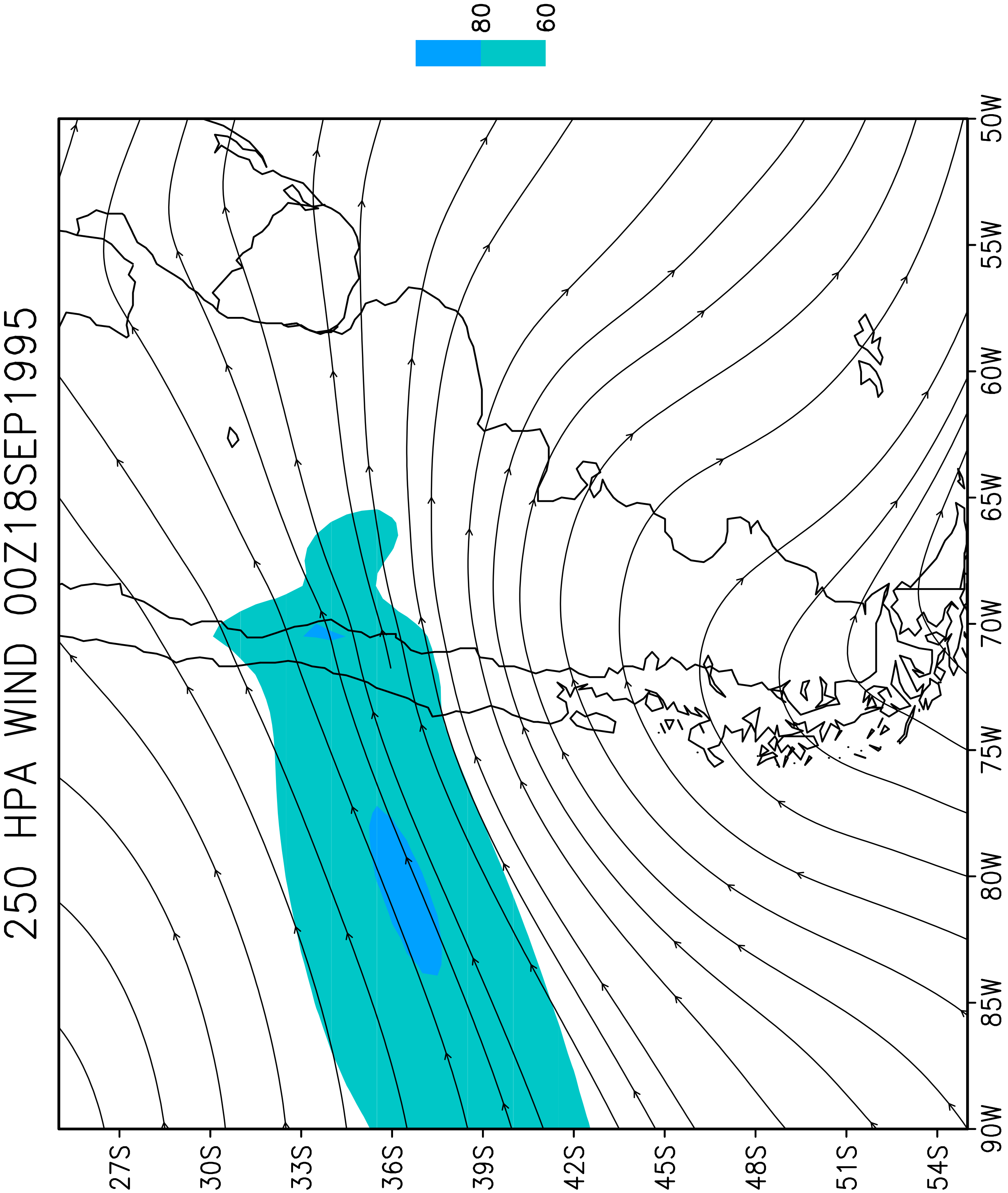

250 HPA WIND 00Z18SEP1995
80
60
27S
30S
33S
36S
39S
42S
45S
48S
51S
54S
50W
55W
60W
65W
70W
75W
80W
85W
90W

Figure

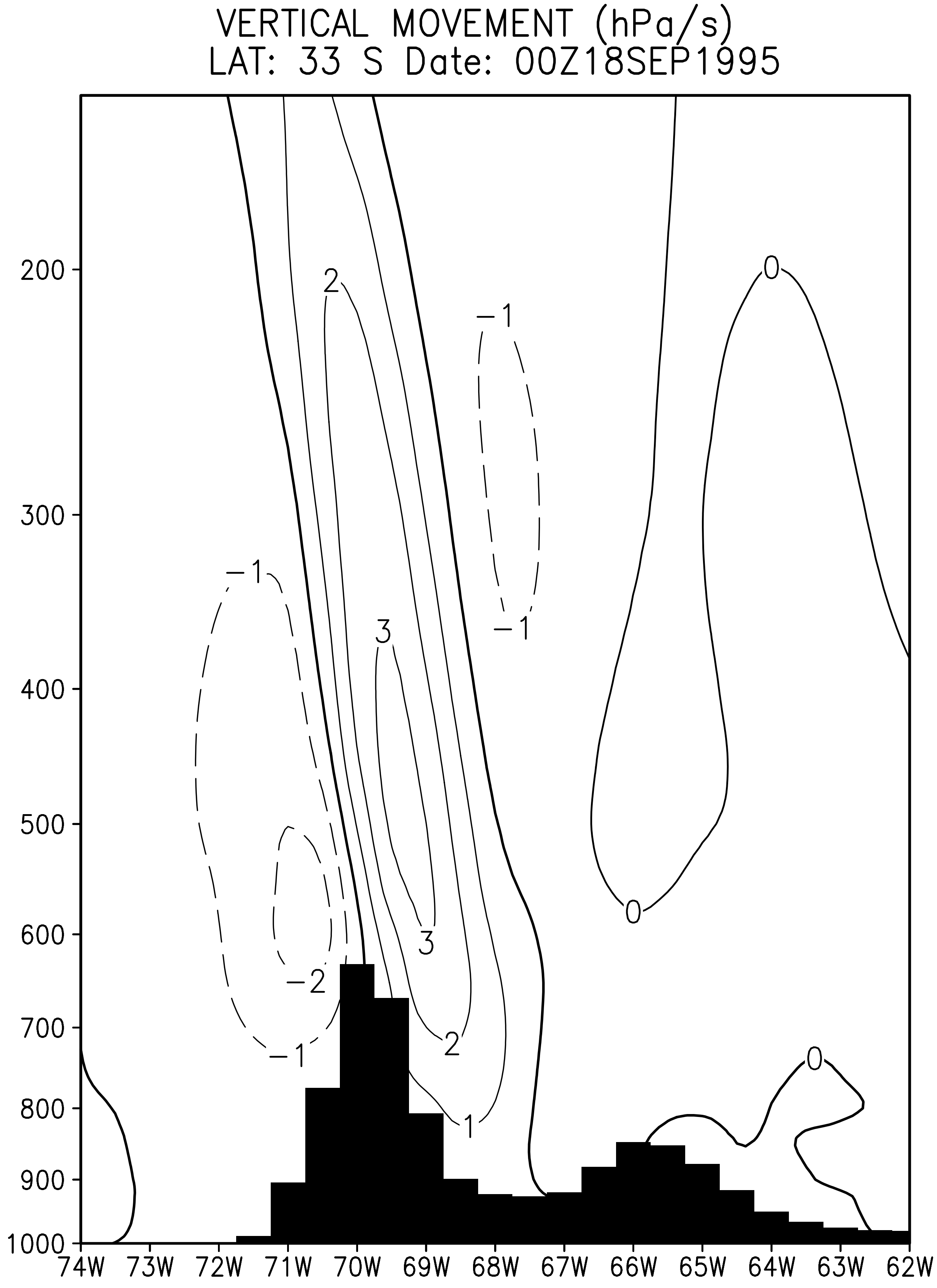
VERTICAL MOVEMENT (hPa/s)
LAT: 33 S Date: 00Z18SEP1995
200
300
400
500
600
700
800
900
1000
74W
73W
72W
71W
70W
69W
68W
67W
66W
65W
64W
63W
62W
0
−1
2
−1
3
−1
0
3
−2
2
−1
0
1

Figure

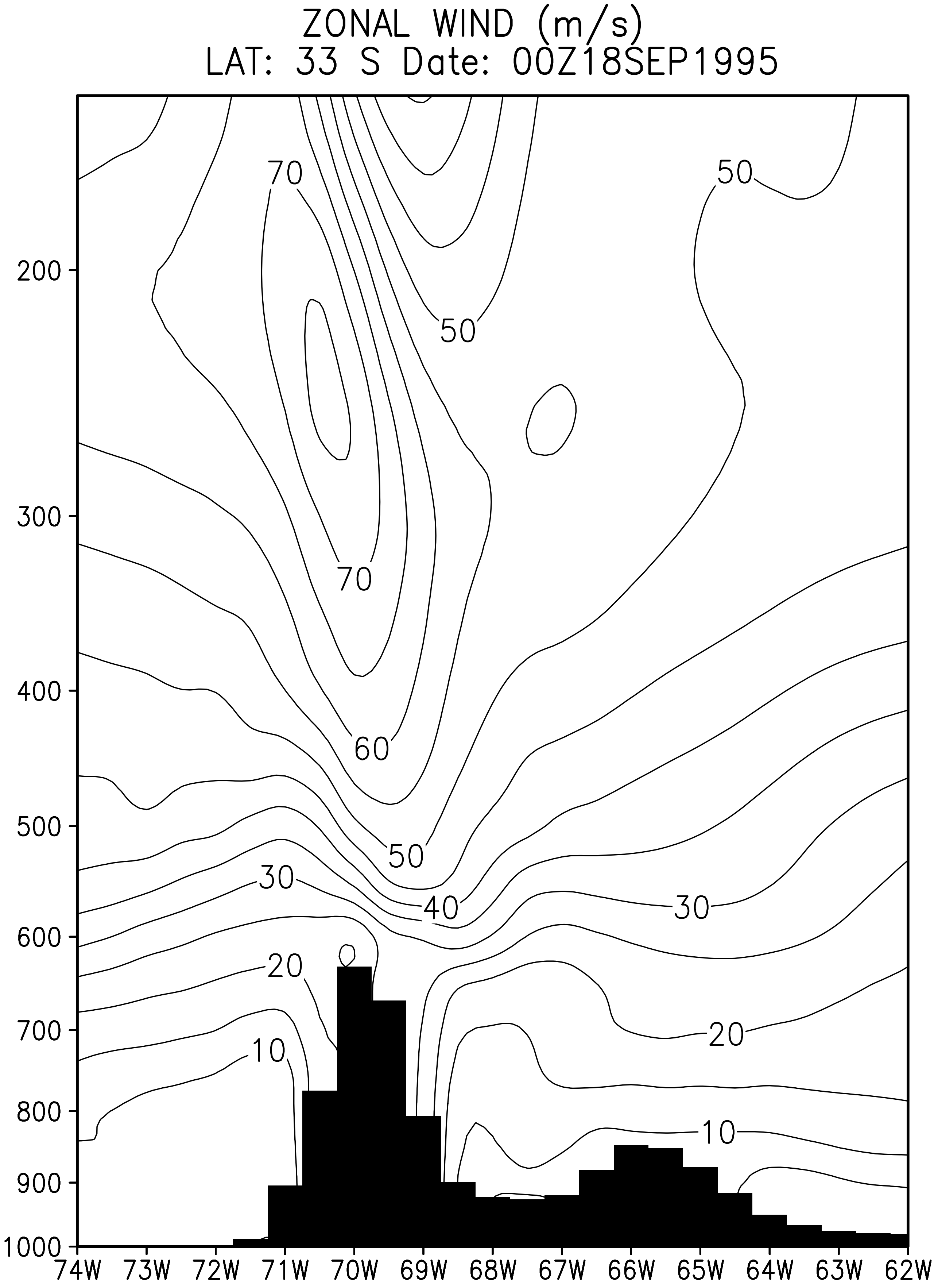
ZONAL WIND (m/s)
LAT: 33 S Date: 00Z18SEP1995
70
50
50
70
60
50
30
40
30
20
20
10
10
200
300
400
500
600
700
800
900
1000
74W
73W
72W
71W
70W
69W
68W
67W
66W
65W
64W
63W
62W

Figure

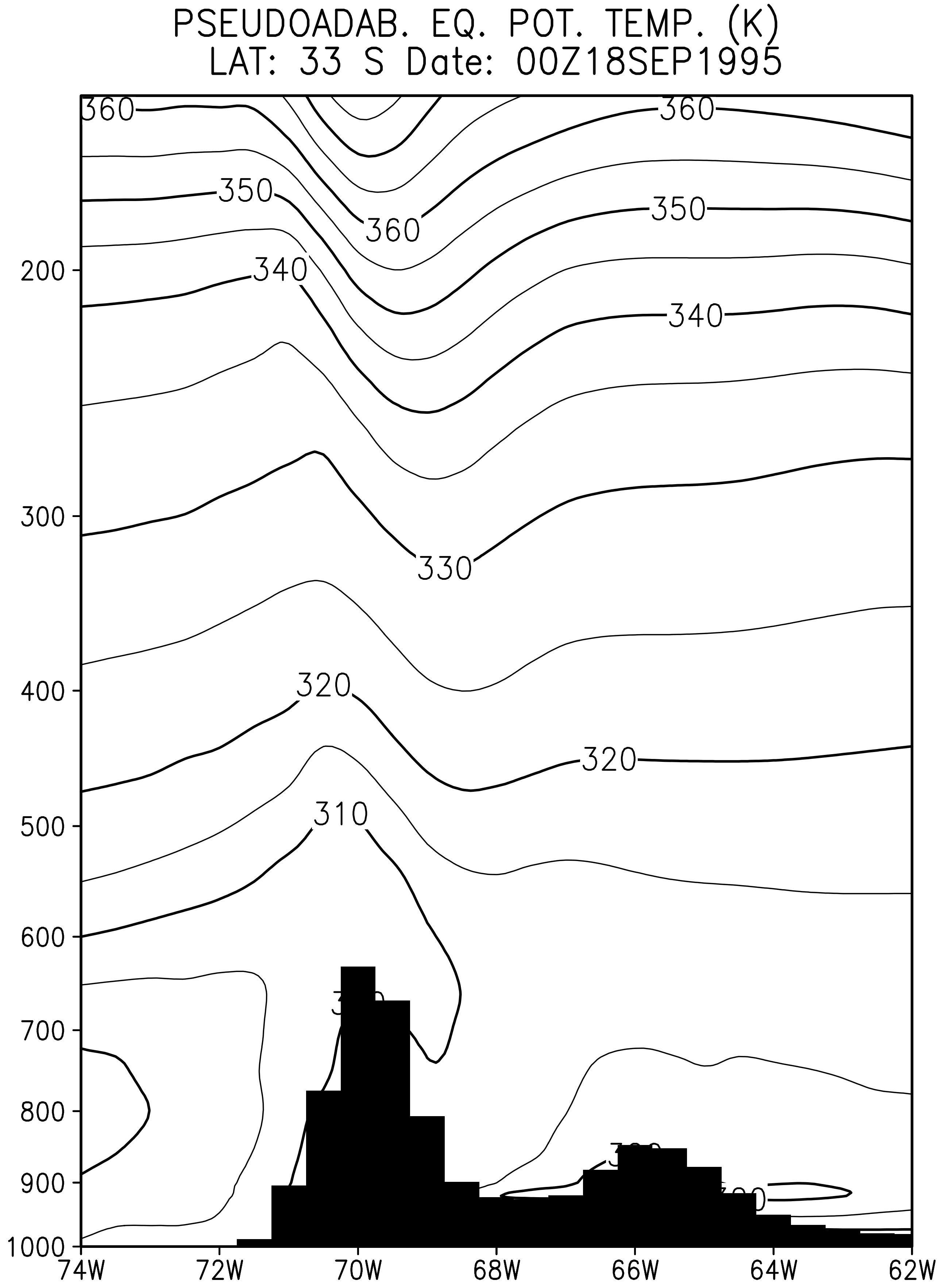

PSEUDOADAB. EQ. POT. TEMP. (K)
LAT: 33 S Date: 00Z18SEP1995
360
360
350
350
360
340
340
330
320
320
310
200
300
400
500
600
700
800
900
1000
74W
72W
70W
68W
66W
64W
62W

Figure

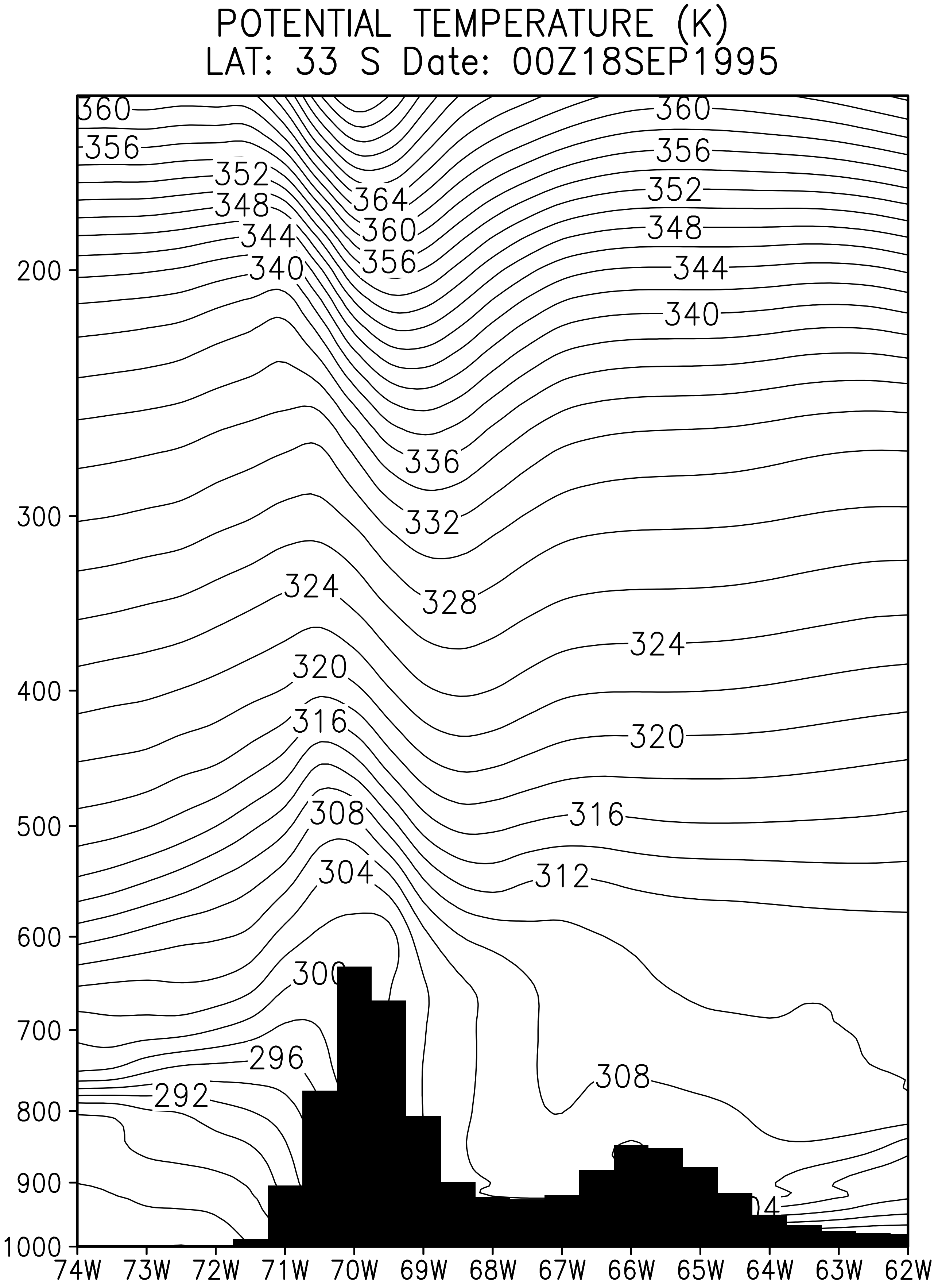
POTENTIAL TEMPERATURE (K)
LAT: 33 S Date: 00Z18SEP1995
360
356
352
348
344
340
364
360
356
336
332
328
324
320
316
308
304
312
300
296
292
308
200
300
400
500
600
700
800
900
1000
74W
73W
72W
71W
70W
69W
68W
67W
66W
65W
64W
63W
62W

Figure

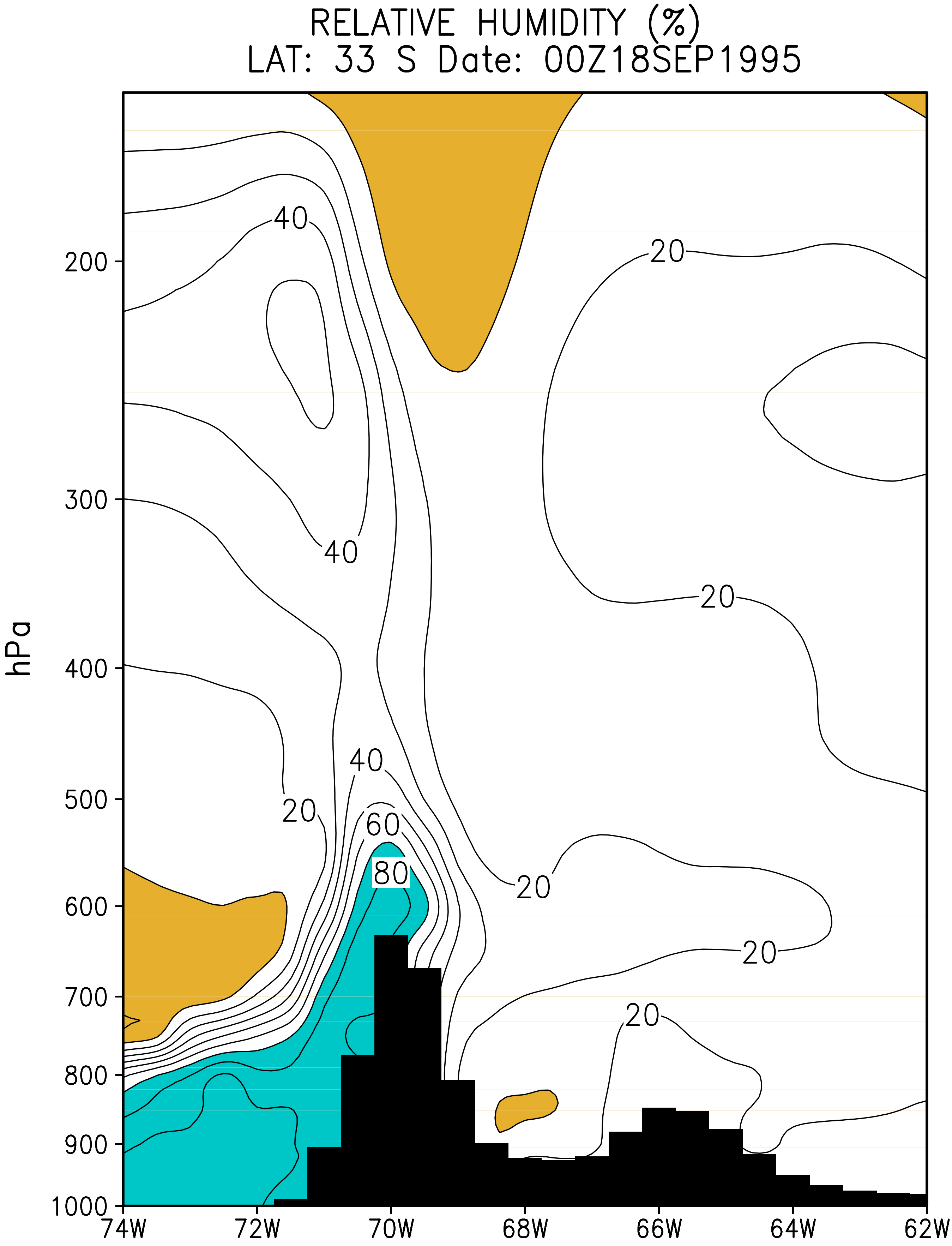

RELATIVE HUMIDITY (%)
LAT: 33 S Date: 00Z18SEP1995
hPa
200
300
400
500
600
700
800
900
1000
74W
72W
70W
68W
66W
64W
62W
20
40
60
80

Figure

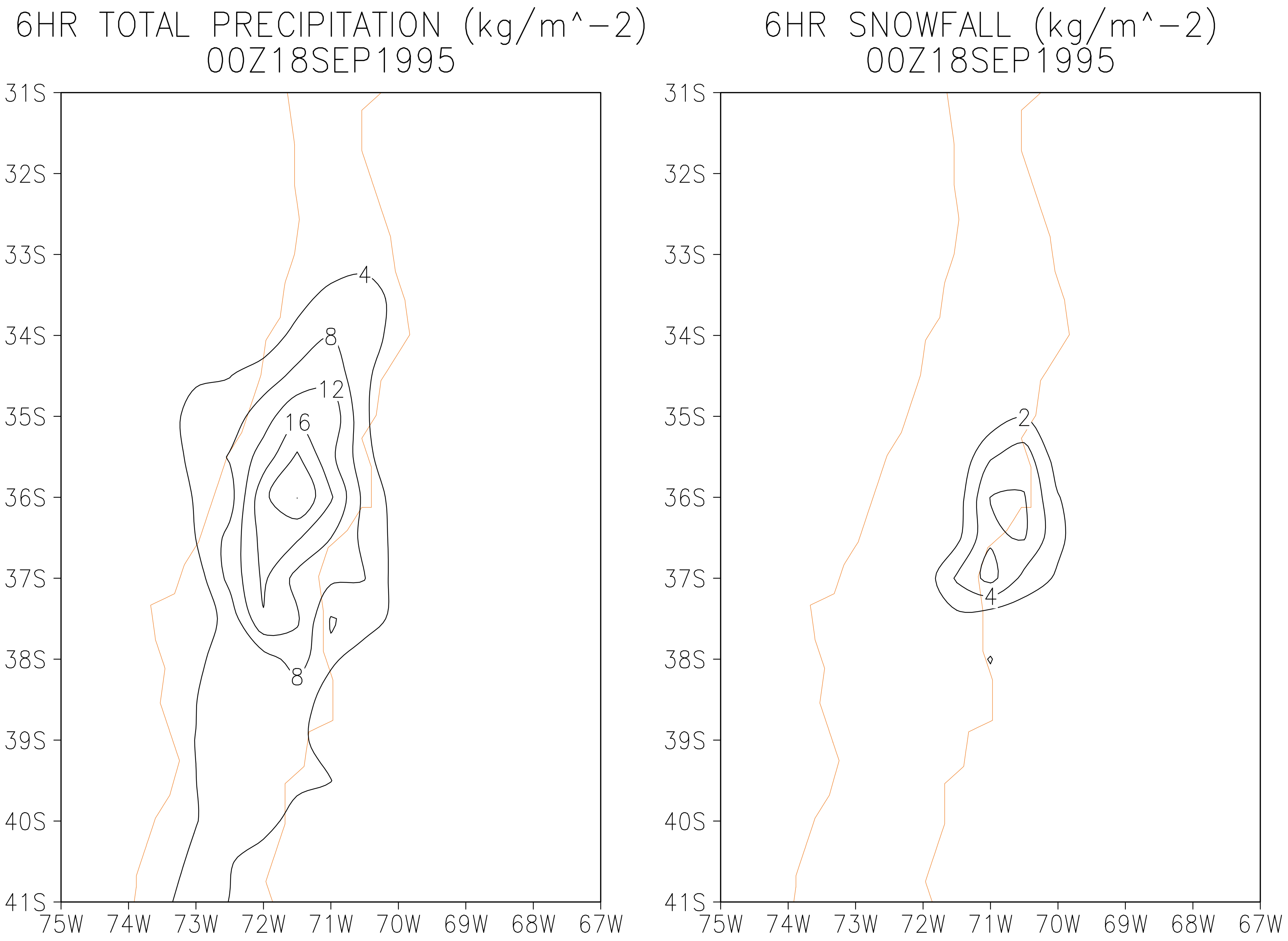
6HR TOTAL PRECIPITATION (kg/m^-2)
00Z18SEP1995
31S
32S
33S
34S
35S
36S
37S
38S
39S
40S
41S
75W
74W
73W
72W
71W
70W
69W
68W
67W
4
8
12
16
8
6HR SNOWFALL (kg/m^-2)
00Z18SEP1995
31S
32S
33S
34S
35S
36S
37S
38S
39S
40S
41S
75W
74W
73W
72W
71W
70W
69W
68W
67W
2
4

Figure

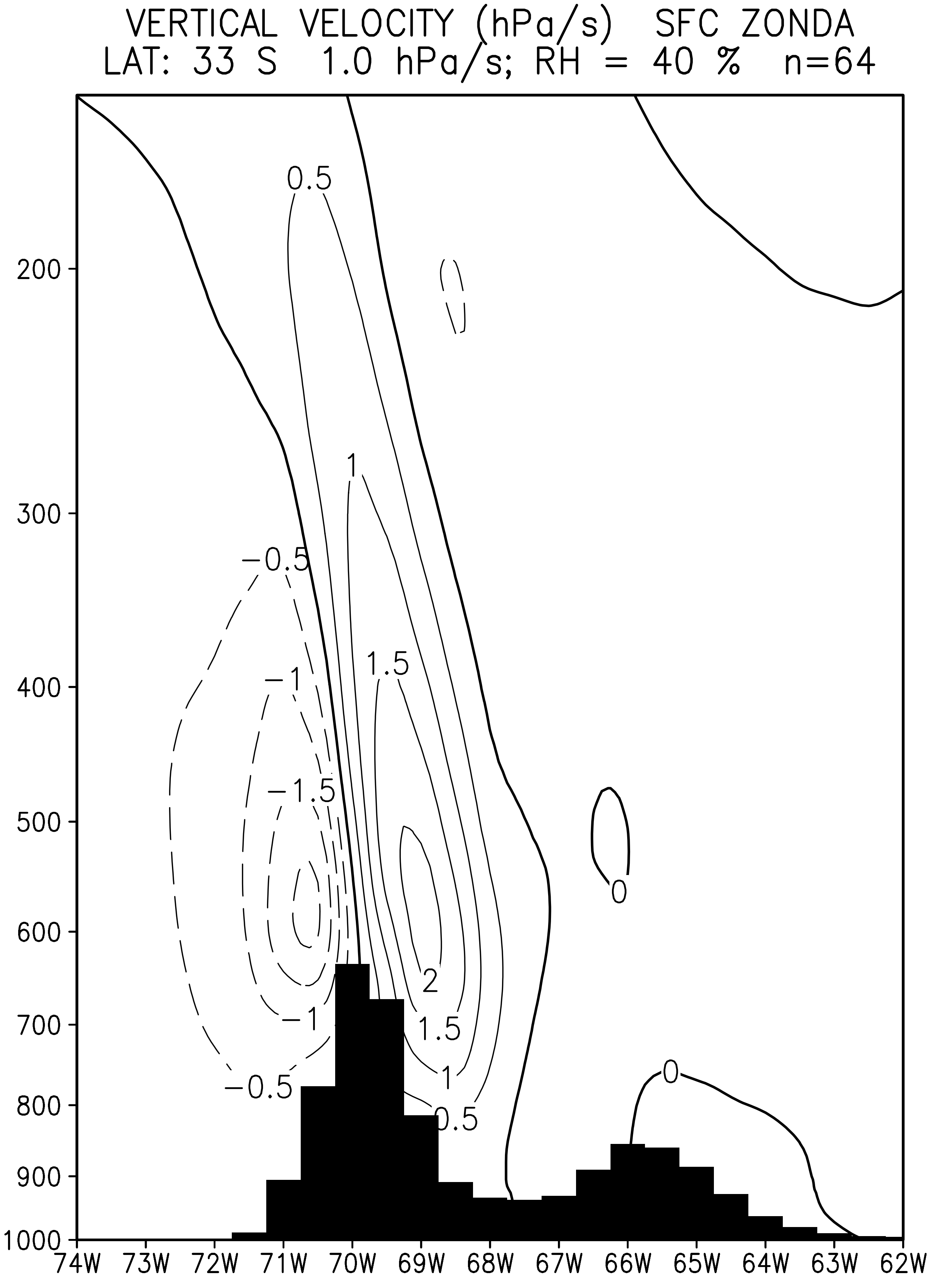

VERTICAL VELOCITY (hPa/s) SFC ZONDA
LAT: 33 S 1.0 hPa/s; RH = 40 % n=64
0.5
1
1.5
2
1.5
1
0.5
−0.5
−1
−1.5
−1
−0.5
0
0
200
300
400
500
600
700
800
900
1000
74W
73W
72W
71W
70W
69W
68W
67W
66W
65W
64W
63W
62W

Figure

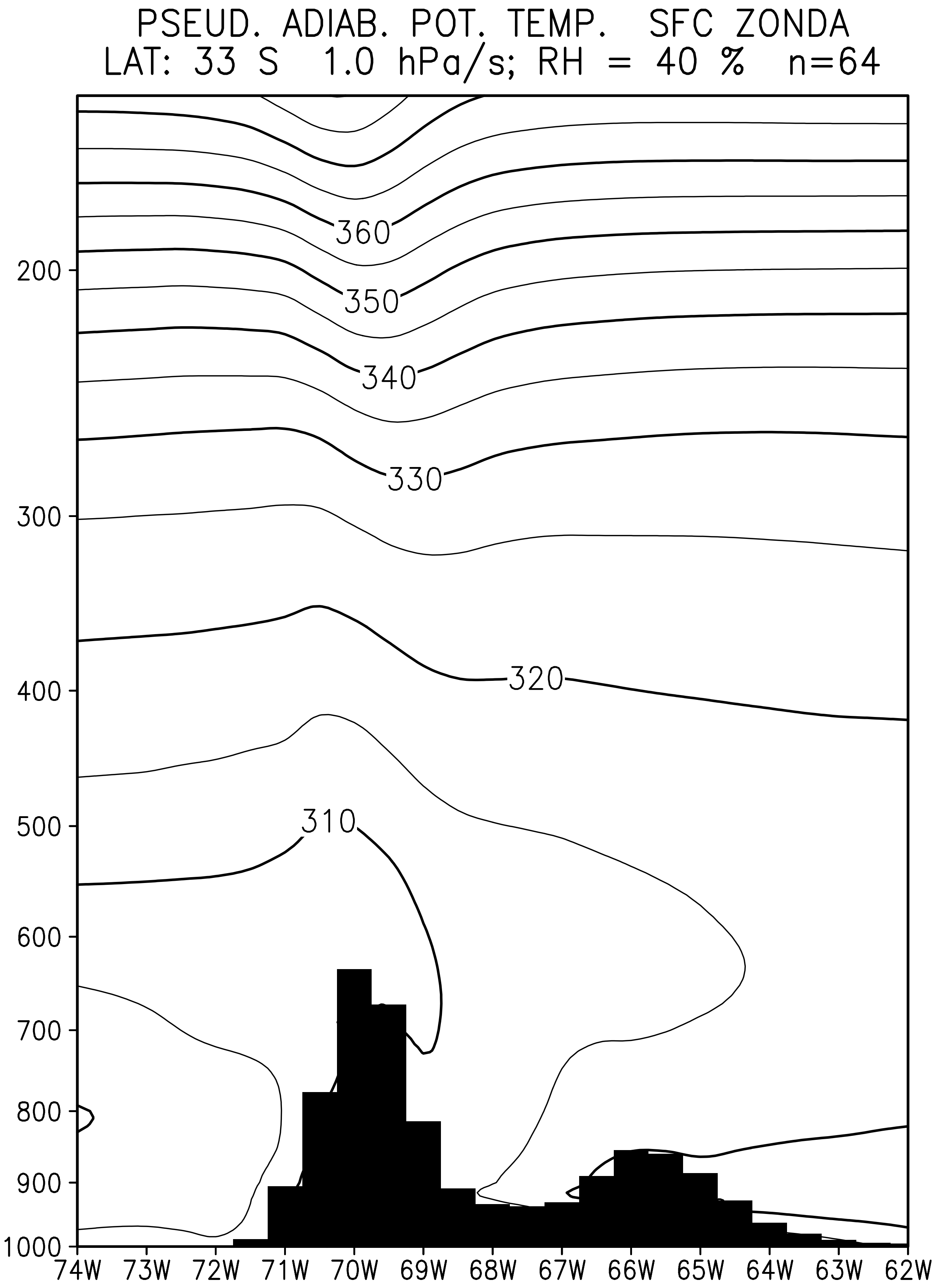
PSEUD. ADIAB. POT. TEMP. SFC ZONDA
LAT: 33 S 1.0 hPa/s; RH = 40 % n=64
360
350
340
330
320
310
200
300
400
500
600
700
800
900
1000
74W 73W 72W 71W 70W 69W 68W 67W 66W 65W 64W 63W 62W

Figure

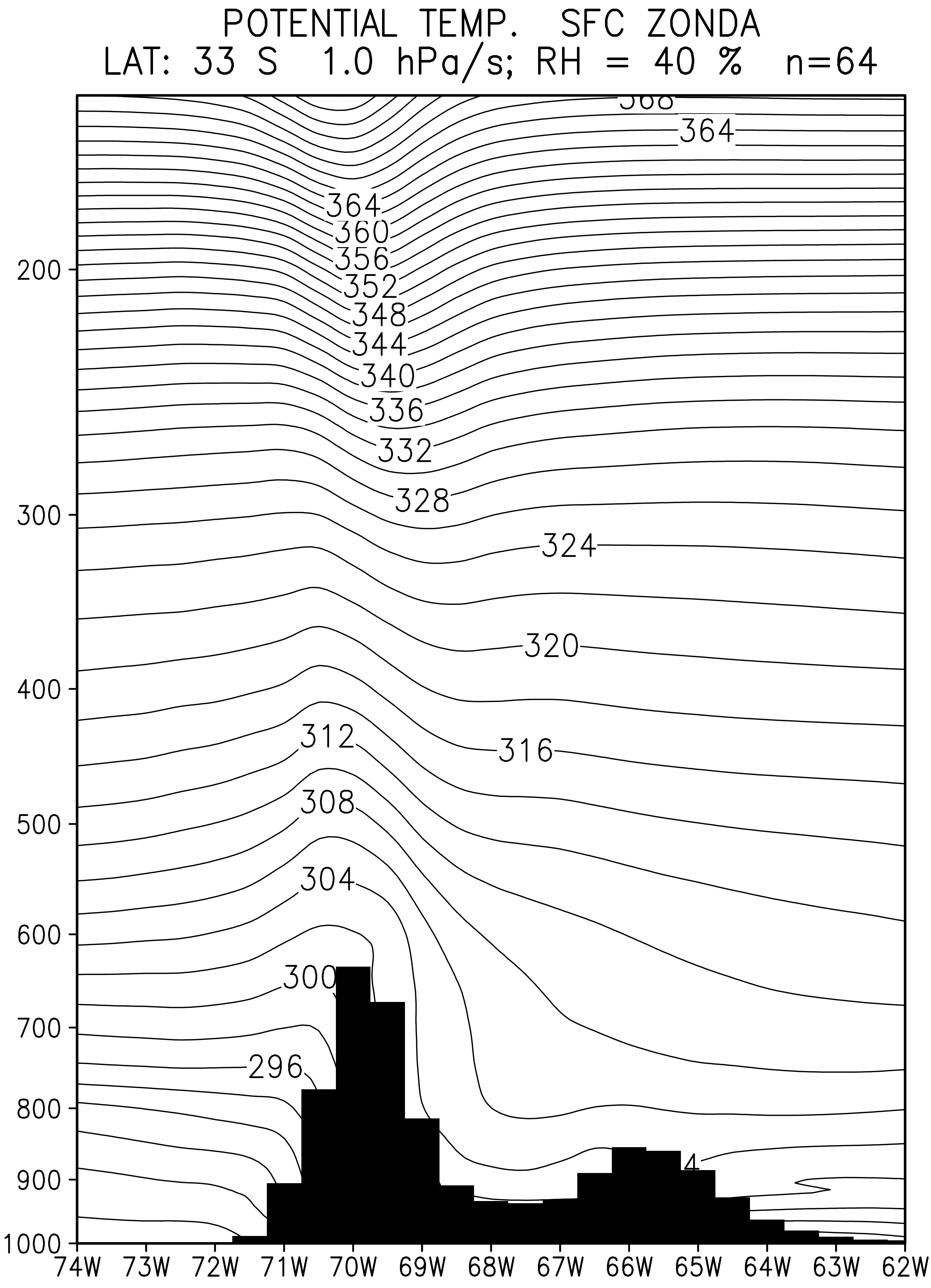

POTENTIAL TEMP. SFC ZONDA
LAT: 33 S 1.0 hPa/s; RH = 40 % n=64
368
364
364
360
356
352
348
344
340
336
332
328
324
320
316
312
308
304
300
296
200
300
400
500
600
700
800
900
1000
74W
73W
72W
71W
70W
69W
68W
67W
66W
65W
64W
63W
62W

Figure

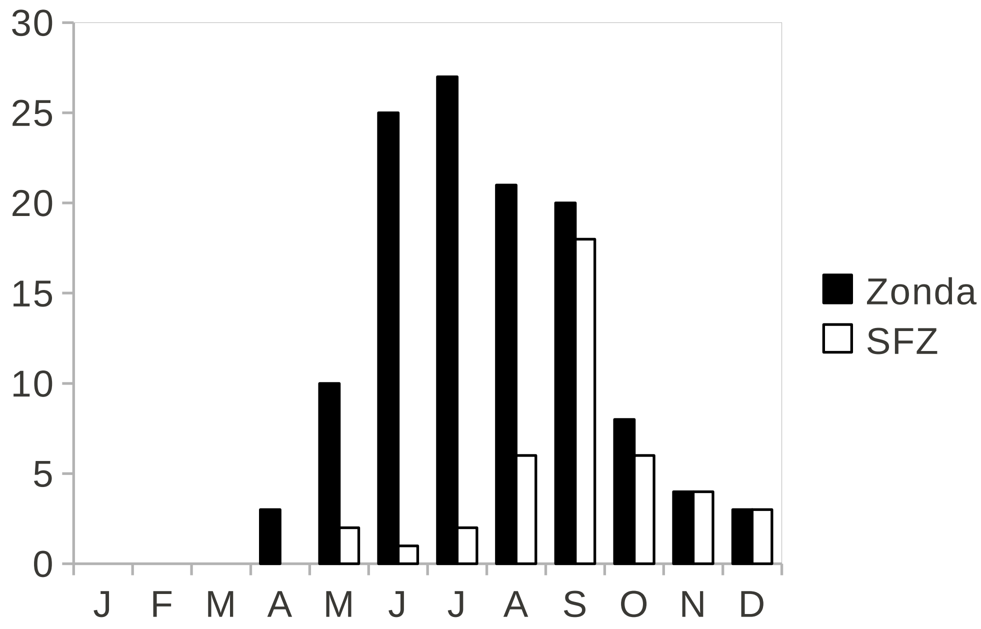

FIGURE 8

Figure

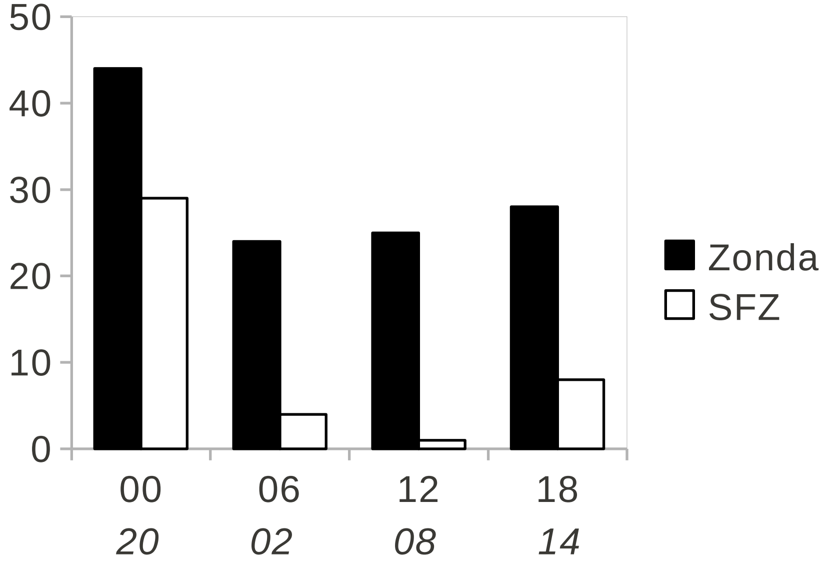

FIGURE 9